International Journal of Pharmaceutics 422 (2012) 495–503

Contents lists available at SciVerse ScienceDirect

International Journal of Pharmaceutics

journal homepage: www.elsevier.com/locate/ijpharm

Pharmaceutical nanotechnology

Drug delivery by polymeric nanoparticles induces autophagy in macrophages

Eidi H.[a], Joubert O.[a], Némos C.[b,e], Grandemange S.[c], Mograbi B.[d], Foliguet B.[e], Tournebize J.[a], Maincent P.[a], Le Faou A.[a], Aboukhamis I.[f], Rihn B.H.[a,*]

[a] Faculté de Pharmacie, EA 3452 CITHEFOR, Nancy-Université, 54001 Nancy Cedex, France
[b] Human Genetics Laboratory, EA 4368, Centre Hospitalier et Universitaire de Nancy, Nancy-Université, Vandoeuvre-Lès-Nancy, Nancy, France
[c] Faculté de Sciences et Technique, EA 4421 SIGRETO, Nancy-Université, Vandoeuvre-Lès-Nancy, Nancy, France
[d] Inserm ERI-21/EA 4319, Faculté de Médecine, University of Nice Sophia-Antipolis, Nice, France
[e] Histology-Embryology-Cytogenetics Department of Faculté de Médecine, Nancy-Université, Vandoeuvre- Lès-Nancy, Nancy, France
[f] Biochemistry Department, Arab European University and Damascus University, Damascus, Syria

ARTICLE INFO

Article history:
Received 9 September 2011
Received in revised form 9 November 2011
Accepted 12 November 2011
Available online 22 November 2011

Keywords:
Nanoparticles
Drug delivery
Autophagy
Apoptosis
Microarray
Mitochondria

ABSTRACT

Drug delivery nanosystems are currently used in human therapy. In preliminary studies we have observed that Eudragit® RS nanoparticles, prepared by nanoprecipitation or double emulsion techniques, are cytotoxic for NR8383 rat macrophages. In this study, we expand our previous analysis and suggest that unloaded Eudragit® RS nanoparticles prepared by nanoprecipitation (NP/ERS) may induce important morphological and biochemical cellular modifications leading to cellular death. In NR8383 rat macrophages cell line exposed to doses varying from 15 to 100 μg/mL, NP/ERS nanoparticles are internalized inside the cells, reach the mitochondria and alter the structure of these organelles. In addition, the exposure to nanoparticles induces cellular autophagy as demonstrated by electron microscopy analysis, microchip array, qRT-PCR and Western blot assays. Although toxicity of nanoparticles has already been evidenced, it is the first time that results show clearly that the toxicity of polymeric nanovectors may be related to an activation of autophagy.

1. Introduction

Nano-drug delivery systems (NDDS) based on polymeric biomaterials have received considerable interest as drug delivery vehicles, and as nonviral gene delivery systems (Unger et al., 2007). Nanoparticles used as drug delivery vehicles are generally <500 nm in at least one dimension, and consist of different biodegradable or non biodegradable materials such as natural or synthetic polymers, lipids or metals (Hoffart et al., 2006; Suri et al., 2007). Despite their wide use, their toxicity is seldom evaluated and the studies are limited, in most cases, to the effect of loaded nanoparticles. On the contrary, the toxicity of the unloaded nanoparticles is not investigated and the mechanisms through which they might interfere with the cellular metabolism are largely unknown. Among the numerous available nanoparticles, those prepared from Eudragit® RS (ERS), a non-biodegradable positively charged copolymer, licensed for clinical use by the major health authorities of Europe, Japan and USA (Hoffart et al., 2006), are efficient NDDS. ERS nanoparticles prepared by nanoprecipitation (NP) or by double emulsion (DE) techniques containing ibuprofen (Pignatello et al., 2002), cyclosporin (Pignatello et al., 2002), indomethacin (Bhardwaj et al., 2010), melatonin (Schaffazick et al., 2008), DNA plasmid (Gargouri et al., 2009) and low molecular weight heparin (Jiao et al., 2002) (LMWH) have been obtained and suggested to be used for the treatment of different pathological conditions. A previous work from our laboratory has already shown, by using MTT and Trypan blue exclusion tests, that unloaded NP/ERS nanoparticles, at a final concentrations ranging from 25 to 400 μg/mL, have cytotoxic effects on the rat macrophage cell line NR8383 (Eidi et al., 2010). Additionally, other studies performed on ERS nanoparticles toxicity are scarce and often they are limited to cell survival (Gargouri et al., 2009; Lamprecht et al., 2006). Taking into consideration that (i) 44% of the total nanoparticles present in a formulation is empty (Eidi et al., 2010); (ii) as demonstrated in rabbits, nanoparticles reach the blood stream after oral administration (Hoffart et al., 2006) and that (iii) macrophages are among the first cells they interact with, we extended our study on the effect of

Abbreviations: CHL, chloroquine; $DCFH_2$-DA, 2′,7′-dichlorofluorescin diacetate; DE, double emulsion; DE/ERS, Eudragit® RS empty nanoparticles prepared by double emulsion technique; ERS, Eudragit® RS PO; GO, gene ontology terms; LPS, lipopolysaccharide; LMWH, low molecular weight heparin; NDA, naphthalene-2,3 dicarboxyaldehyde; NDDS, nano drug delivery systems; NP, nanoprecipitation; NP/ERS, Eudragit® RS PO empty nanoparticles prepared by nanoprecipitation technique; SWCNTs, single-walled carbon nanotubes; SDS, sodium dodecyl sulfate; SEM, scanning electron microscopy; TEM, transmission electronic microscopy.

* Corresponding author at: Faculté de Pharmacie, 5 rue Albert Lebrun, BP 80403, 54001 Nancy Cedex, France. Tel.: +33 0383 682 355; fax: +33 0383 682 301.
E-mail addresses: bertrand.rihn@pharma.uhp-nancy.fr, housam.eidi@gmail.com (B.H. Rihn).

0378-5173/$ – see front matter © 2011 Elsevier B.V. All rights reserved.
doi:10.1016/j.ijpharm.2011.11.020

NP/ERS on NR8383 rat macrophages, which evolve in fully activated macrophages (Nguea et al., 2008), with the aim to better elucidate the molecular mechanisms that may be responsible of the observed cytotoxicity and so to further address the safety issues surrounding nanoparticles use.

2. Materials and methods

2.1. Materials

Eudragit® RS PO (ERS; MW = 150,000 Da) was a gift of Evonik polymers (Darmstadt, Germany). CAS number: 33434-24-1, chemical/IUPAC name: poly(ethyl acrylate-co-methyl methacrylate-co trimethylammonioethyl methacrylate chloride) 1:2:0.1. INCI name: Acrylates/Ammonium Methacrylate Copolymer, molecular weight: 32 g/mol. Eudragit® RS PO was described in the following monographs: (i) European pharmacopoeia: Ammonio Methacrylate Copolymer, Type B; (ii) USA pharmacopoeia: Ammonio Methacrylate Copolymer, Type B – NF; (iii) Japanese pharmacopoeia: Aminoalkyl Methacrylate Copolymer RS. Pluronic® F68 [CAS number: 11104-97-5] (Saint-Quentin Fallavier, France) was used as surfactant for particle preparations. Reduced glutathione (GSH), naphthalene-2,3- dicarboxyaldehyde (NDA), 2′,7′-dichlorofluorescin diacetate ($DCFH_2$-DA) and dichlorofluorescein (DCF) were purchased from Sigma–Aldrich (France).

2.2. Methods

2.2.1. Nanoparticle preparation

Nanoparticles were prepared by nanoprecipitation as previously described (Bodmeier et al., 1991; Fessi and Puisieux, 1989). Briefly, 300 mg of polymer were dissolved in 15 mL of acetone (organic phase). The solution was poured in a glass syringe, and flowed slowly under stirring, in 40 mL of a Pluronic® F68 (0.5%, w/v) aqueous solution. The solvent was removed by rotary evaporation under vacuum at 40 °C (Heidolph, Schwabach, Germany) and the solution concentrated to 15 mL.

2.2.2. Particle size measurement

Particle sizes were estimated by photon correlation spectroscopy (PCS) using a Zetasizer™ (Malvern Instruments Worcestersher, UK). Each sample was diluted with filtrated bidistilled water until the appropriate concentration of particles was achieved to avoid multiscattering events. Using cumulative analysis software and exponential sampling method, particle size (*z*-average) and polydispersity index of equivalent hydrodynamic spheres were determined using the results of three determinations.

2.2.3. Zeta potential measurement

Particle electrophoretic mobility was determined three times for each sample by laser Doppler anemometry in a microelectrophoresis cell of Zetasizer™.

2.2.4. Scanning electron microscopy (SEM)

Briefly, nanoparticles deposited on a plastic coverslip (Thermanox, 174950, Merck Eurolab, Strasbourg, France) were dehydrated by increased ethanol concentrations (25°, 50°, 70°, 90°, and 100°) and treated with hexamethyldisilazane for 10 min at room temperature. The coverslips were coated with gold. Preparations were observed under SEM (Stereoscan 240 S/N, Léo, Rueil-Malmaison, France) at less than 20 kV.

2.2.5. Cells and cell culture

The NR8383 rat alveolar macrophage cell line was purchased from the American Type Culture Collection (CRL-2192, ATCC, Manassas, VA). Cells were grown as 50% adherent and 50% floating cells in Dulbecco's modified Eagle's medium (DMEM: GIBCO Invitrogen, Cergy Pontoise, France) supplemented with 15% fetal calf serum (FCS, Eurobio, Les Ullis, France), 200 mM L-glutamine (G7513, Sigma–Aldrich, Saint Quentin Fallavier, France) and antibiotic (A5955, Sigma–Aldrich, Saint Quentin Fallavier, France) at 37 °C under 5% CO_2. Cells were treated with nanoparticles using this culture medium in all the following experiments.

2.2.6. Transmission electron microscopy (TEM)

Briefly, NR8383 cells were treated with 15 and 25 μg/mL of NP/ERS for 2 h, then they were immediately fixed with ice-cold 3% glutaraldehyde for 3 h. Cells were then post-fixed in 1% OsO_4 for 1 h at 4 °C, progressively dehydrated by increasing concentrations of ethanol and finally treated with propylene oxide and included in resin semi-fine (1.5 μm) and ultra-fine sections (70–90 nm) were prepared with an ultra-microtome (Reichert-Yung) and examined with the electron microscope Philips CM12 (FEI Electron Optics, Eindhoven, The Netherlands).

2.2.7. Total RNA extraction

Total RNA was extracted from cells, treated with 15 and 100 μg/mL of NP/ERS for 24 h, using RNeasy Mini Kit (QIAGEN, Courtaboeuf, France) following manufacturer instructions. RNA purity and concentration were determined spectrophotometrically using a NanoDrop ND-1000 (NanoDrop Technologies, Wilmington, DE).

2.2.8. Microarray

Microarray experiments were performed following the MIAME (Minimal Information About a Microarray Experiment) criteria (Brazma et al., 2001). Briefly, RNA samples were extracted from NR8383 cells and melted at 65 °C. cDNA was then synthesized using M-MLV reverse transcriptase (RT) (EC 2.7.7.6.9, Invitrogen, Cergy Pontoise, France). The cDNA was transcripted to cRNA using T7 RNA polymerase and labeled with fluorescent Cyanine 3-CTP. The cRNA (350 ng) was amplified and labeled using One-Color Gene Amp Labeling Kit (Agilent Technologies, Massy, France) following manufacturer's instructions, then purified using RNeasy Mini Kit (QIAGEN, Courtaboeuf, France) and quantified spectrophotometrically using a NanoDrop ND-1000 (NanoDrop Technologies, Wilmington, DE). The One-Color Spike-In Kit (Agilent Technologies, Massy, France) was used to provide positive controls. Before the hybridization step, 1.65 μg of cRNA was fragmented using the Gene Expression Hybridization Kit (Agilent Technologies, Massy, France) by incubation with fragmentation buffer and 10× blocking agent for 30 min at 60 °C. Fragmented cRNA was hybridized to Agilent 4× 44 K Whole Rat Genome Microarray (Agilent Technologies, Massy, France) using hybridization chambers (Agilent Technologies, Massy, France) and hybridization oven (Agilent Technologies, Massy, France) for 20 h at 65 °C. One-minute wash was performed twice using wash solution 1 and 2, respectively (Agilent Technologies, Massy, France). Microarrays were stabilized and dried by acetonitrile (Sigma–Aldrich, Saint Quentin Fallavier, France). The slides were scanned with the Agilent Microarray Scanner (Agilent technologies, Palo Alto, CA, USA) and the scanned images were extracted using Feature Extraction Software version 9.5.3 (Agilent). Analysis was performed with Genespring GX10 (Agilent Technologies, Palo Alto, CA, USA).

2.2.9. RNA reverse transcription and quantitative RT-PCR (qRT-PCR)

Total RNA (1 μg) from control or treated cell samples were reverse-transcripted with 50 nmol of oligo (dT) using M-MLV reverse transcriptase (RT) [EC 2.7.7.4.49, Invitrogen, Cergy Pontoise, France] following manufacturer's protocol. qRT-PCR was

Table 1
Primers sequences used in qRT-PCR experiments.

Primers	Sens	Anti sens
s18	5′-CGCCGCTAGACGTAGAATTCT-3′	5′CATTCTTGGCAAATGCTTTGC-3′
nfκb2	5′-TTCGGAACTGGGCAAATGTT-3′	5′-ACACGTAGCGGAATCGAAAT-3′
opa1	5′-TCCTGTGCATTCAAGATGGA-3′	5′-GAGCTTTCATTGGGAAGAGC-3′
tnf	5′-TAGCCCACGTCGTAGCAAAC-3′	5′-TGGTATGAAATGGCAAATCG-3′
bcl2l13	5′-TGGGATGCCTTTGTGGAACTAT-3′	5′-GGTCTGCTGACCTCACTTGT-3′
casp8	5′-GGTTTCTGCCTACAGGGTTA-3′	5′-TCGTAATCGTCGATCCTTCC-3′
pdcd4	5′-GGTGTGCCCGTGTTGGCAGT-3′	5′-GGCCCACCAATCGTGGTGCT-3′
ncf1	5′-TTCACAACTACGCAGGTGAA-3′	5′-TTATCTCCTCCCCAGCCTTC-3′
atg16l1	5′-CTTGTAATTCCCGCATTGCT-3′	5′-GCCTCGTATGTCTTTGATGC-3′

performed with a Stratagene Mx3000p system and Mesa Green qPCR MasterMix Plus for SYBR® (RT-SY2X-03-WOULR, Eurogentec, Belgium). Briefly, 100 ng of reverse-transcripted RNA from each sample were mixed with appropriate concentrations of tested gene primers (Table 1) and the Mesa Green qPCR MasterMix. *MRPSI8A* (*s18*) was used as internal control gene. PCR amplifications were carried out as follows: 5 min at 95 °C; 45 cycles (15 s at 95 °C, 40 s at 60 °C and 40 s at 72 °C). A standard curve was made for each gene and the subsequent slope was used to calculate the PCR reaction efficiency ($E = 10^{(-1/\text{slope})}$). For each sample, the gene expression level was calculated from the threshold cycle (C_t), which is the number of cycles necessary for the first detection of a PCR product.

2.2.10. Western blot

Total proteins (25 μg) from NR8383 cells either exposed (25 and 100 μg/mL of NP/ERS for 4, 10, 24, 36, 48 and 72 h) or not to nanoparticles were run on SDS-polyacrylamide gels (10%) as previously described (Corcelle et al., 2006; Laemmli, 1970) and transferred onto a PVDF membrane, followed by immunoblot analysis using monoclonal antibodies directed against anti-cleaved PARP (cat #552596, BD Biosciences Pharmingen, France), anti-p65 (cat #sc7178, Santa Cruz Biotechnology, France), mouse anti-OPA1 (cat #612606, BD Transduction Laboratories, France), anti LC3-II (clone 5F10; Nanotools, France), anti-actin (cat #C-11, Santa Cruz Biotechnology, France) or anti-tubulin (Santa Cruz Biotechnology, France) at the optimized dilutions. Bands were detected using an IgG polyclonal anti-mouse antibody conjugated to peroxidase (EC 1.11.1.7; Sigma) after addition of a chemiluminescent substrate (Roche).

2.2.11. Immunofluorescence

Cells were treated with either NP/ERS (0, 25, 50 and 100 μg/mL for 4 h) or chloroquine (CHL) CAs # [58175-87-4] as a positive control of autophagy (30 μM, 4 h). Cells deposited on a glass coverslip were fixed for 15 min in 4% paraformaldehyde in PBS at 4 °C and washed in PBS. Nonspecific binding was blocked with 1% bovine serum albumin–PBS for 15 min. Anti-LC3 antibody (1/100) was applied overnight at 4 °C. After two washes with PBS, sections were incubated with FITC-conjugated anti-mouse secondary antibody for 1 h at room temperature. The preparations were examined under a confocal laser-scanning microscope (Zeiss LSM510 Meta™) fitted with a 405 and 488 krypton/argon laser for simultaneous detection of DAPI and FITC fluorescence.

2.2.12. Intracellular reduced glutathione (GSH) measurement

Reduced glutathione measurements were performed as previously described (Lewicki et al., 2006), with some modifications. Briefly, cells were dispensed (5×10^5 cells/well) into a 6-well microplate. Cells were incubated with 25 and 100 μg/mL of NP/ERS for 24 h. Then, cells were washed three times with PBS solution (pH 7.4), and 1 mL of lysis solution [0.5 M perchloric acid, 0.1 M HCl and 2 mM EDTA] was added to cells. In order to remove the precipitated protein, cell lysates were centrifuged at 10,000 × *g* at 4 °C for 15 min. 60 μL of supernatant, 120 μL of borate buffer (0.4 M, pH 9.2) and 20 μL of naphthalene-2,3- dicarboxyaldehyde (NDA) solution in ethanol were mixed in a 96-black well microplate and incubated in the dark at 4 °C for 25 min. Fluorescence intensity was then measured at 485-nm excitation and 528-nm emission using a microplate reader (Biotek Synergy). Results were expressed as nmol of GSH per mg of protein. Total protein quantity in cell lysate was determined by the Lowry method (Lowry et al., 1951).

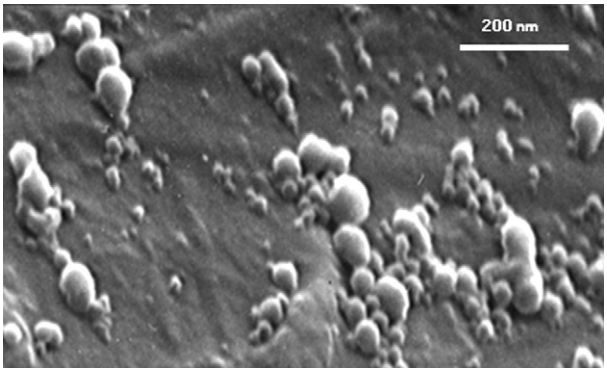

Fig. 1. SEM observation of NP/ERS nanoparticles.

2.2.13. Intracellular ROS measurement

The production of intracellular reactive oxygen species (ROS) was measured using an oxidation-sensitive fluorescent probe, 2′,7′-dichlorofluorescin diacetate ($DCFH_2$-DA) (Wang and Joseph, 1999). $DCFH_2$-DA passively enters the cell where it reacts with ROS to form a highly fluorescent compound, namely the dichlorofluorescein (DCF). Briefly, cells were dispensed (5×10^5 cells/well) into a 6-well microplate. Cells were exposed to 25 and 100 μg/mL for 24 h of NP/ERS. Lipopolysaccharide (LPS) was used as a positive control of ROS production (1 μg/mL for 24 h). Cells were washed three times with PBS solution (pH 7.4), resuspended in 1 mL of 4 μM $DCFH_2$-DA solution and incubated for 40 min at 37 °C. Cells were lysed using a lysis buffer (0.5 M Tris–HCl, 1.5 M NaCl, 3.5 mM SDS, 16 mM Triton X-100 and 1× protease inhibitor cocktail). The conversion of DCFH to the fluorescent product (DCF) was measured using a microplate reader (Biotek Synergy) with 485-nm excitation and 528-nm emission. ROS production was quantified from a DCF standard curve and results were expressed as DCF concentration (nM).

2.2.14. Statistical and data analysis

Microarray data and statistics were analyzed using GeneSpring GX10 software. Regarding qRT-PCR and array results, genes which showed more than a 2-fold or less than 0.5-fold intensity as compared to control, were considered respectively as up- or down-regulated (Lin et al., 2003). In our study, the differences between the control and the experimental group were evaluated with the one-paired *t*-test. *p*-Values ≤0.01 were considered as significant.

3. Results

3.1. Nanoparticle characterization

NP/ERS nanoparticles were positively charged (+40.6 ± 5 mV) owing to the quaternary ammonium groups of the polycationic ERS polymer. In addition, these nanoparticles had a mean nominal diameter value of 54.2 ± 6 nm and a weak polydispersity index (0.5 ± 0.04). Particle size results obtained by Zetasizer™ were comparable to those measured by SEM analysis (Fig. 1).

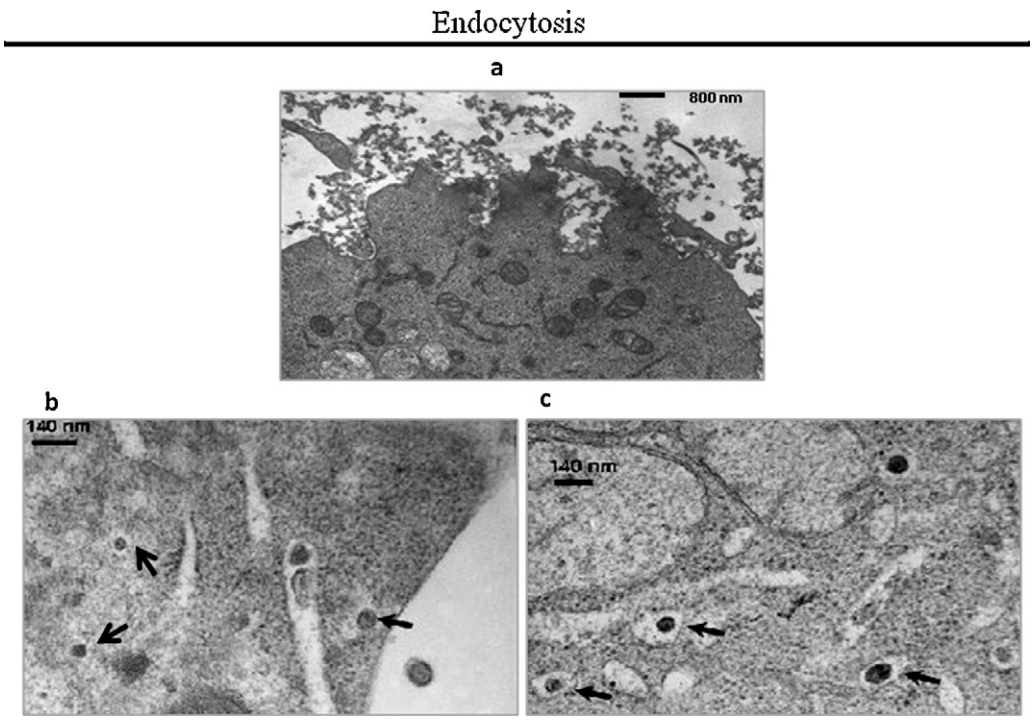

Fig. 2. Nanoparticle uptake by NR8383 macrophages. Macrophages exposed for 2 h to nanoparticles at a final concentration of 25 μg/mL (a) and 15 μg/mL (b and c). Arrows indicate internalized nanoparticles (a).

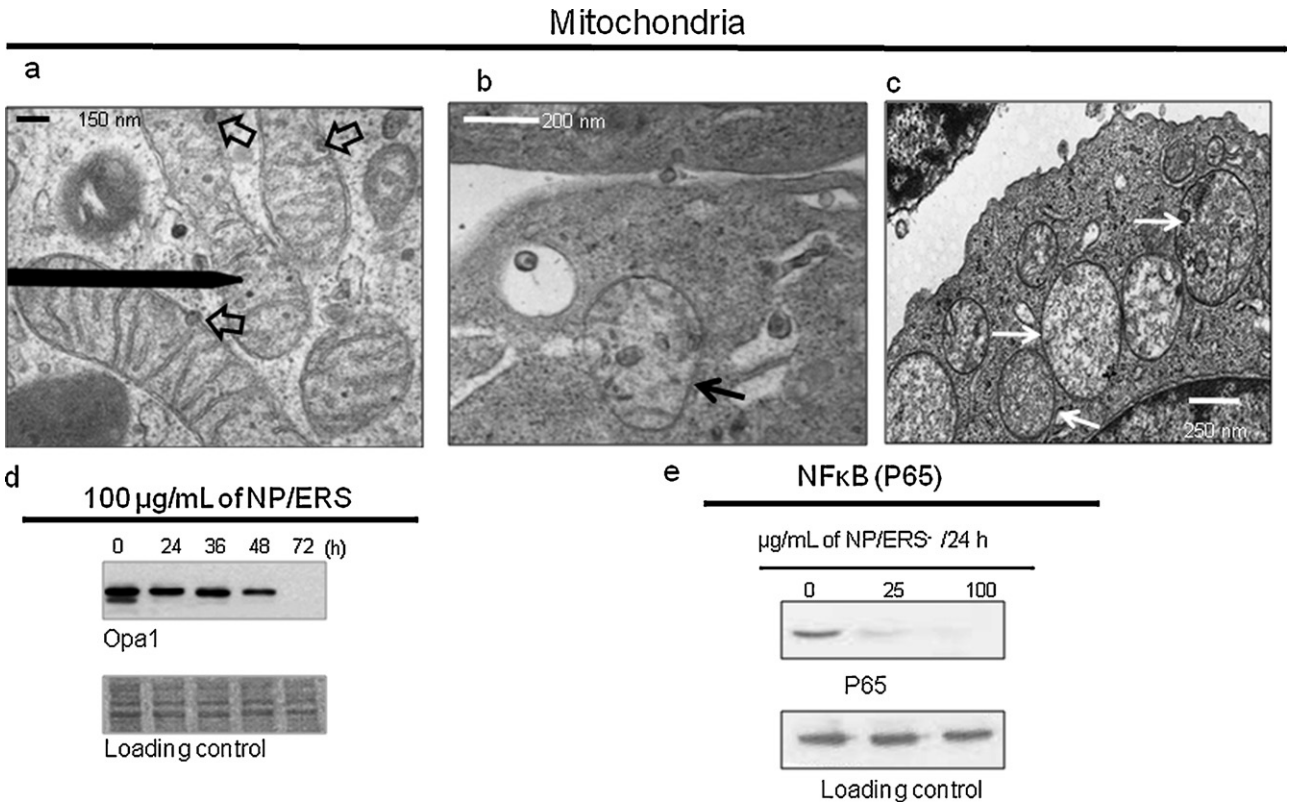

Fig. 3. Mitochondria are the intracellular target of NP/ERS nanoparticles. (a) Macrophages exposed to 15 μg/mL of nanoparticles for 1 h. Arrows indicate internalized nanoparticles into the cells and present on the border or inside the mitochondria. (b and c) Particle in an endosome and disorganization of *cristae* structure of mitochondria, cells were treated with 15 and 50 μg/mL of NP/ERS for 1 and 6 h, respectively. (d) and (e) Western blotting: (d) time-dependent down regulation of OPA1, (e) effect of nanoparticle concentration on the down regulation of NfκB (loading control is stained with Red Ponceau).

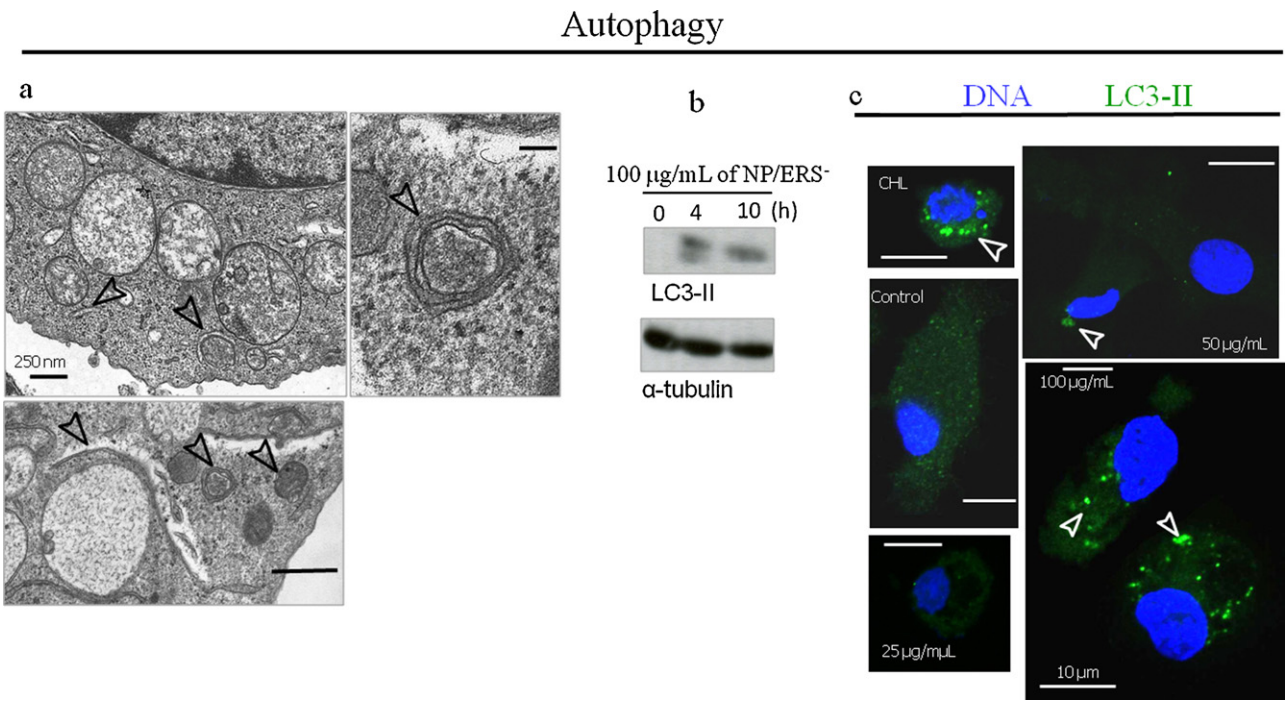

Fig. 4. Autophagy induced by NP/ERS particles. (a) Cells exposed to 50 µg/mL of nanoparticles for 6 h. Arrows indicate accumulation of double- and multi-membrane phagophores as well as lamellar autophagosomes. Note the dense aspect of mitochondria. (b) LC3-II protein levels obtained by Western blotting. No LC3-II protein was evidenced in control cells. Cells were exposed to 100 µg/mL of nanoparticles for 4 and 10 h, respectively. α-Tubulin was used as loading control. (c) In vitro accumulation of LC3-positive vesicles in NR8383 cells treated with NP/ERS observed by confocal fluorescence microscopy. Arrows indicate LC3-positive vesicles (green fluorescence). The blue fluorescence corresponds to DNA (stained with DAPI). (For interpretation of the references to color in the figure caption, the reader is referred to the web version of the article.)

3.2. TEM observations

Uptake of particles occurred in NR8383 macrophages upon incubation for 2 h with nanoparticles at a final concentration of 15 and 25 µg/mL. The particles were inside endosomes, free in the cytoplasm (Fig. 2a–c) or in contact with mitochondria. Some particles were inside those organelles, associated to their inner membrane (Fig. 3a). Alteration in the structure of mitochondria and disorganization of the *cristae* were also noted (Fig. 3b and c). When exposed to higher doses, namely 50 µg/mL for 6 h, cells displayed additional modifications characteristic of autophagy such as phagophore and autophagosome formation (Fig. 4a).

3.3. Microarray result analysis

Cells exposed to 25 µg/mL or 100 µg/mL nanoparticles had 56 and 427 transcripts significantly and differentially expressed as compared to unexposed cells. Several down or up regulated genes were associated with autophagy, G-protein signaling pathway, apoptosis and oxidative stress (Table 2). The effect was dose dependent

Table 2
Incidence of nanoparticles on gene expression as measured by microarray analysis. Only genes showing a significant up or down regulation are noted ($p \leq 0.01$).

	Approved gene symbol	Fold change in gene expression ± SD		HUGO approved gene name
		25 µg/mL	100 µg/mL	
GO[a]:0006915, apoptosis	*pdcd4*	−2.46 ± 0.08	−4.16 ± 0.09	Programmed cell death 4 (neoplastic transformation inhibitor)
	bcl2l13	–	−2.18 ± 0.05	BCL2-like 13 (apoptosis facilitator)
	bfar	–	−2.13 ± 0.04	Bifunctional apoptosis regulator
	casp8	–	−2.00 ± 0.03	Caspase 8
	rtkn	–	+2.08 ± 0.07	Rhotekin
	opa1	–	−2.23 ± 0.03	Optic atrophy 1 (autosomal dominant)
	tnfrsf5	–	+2.26 ± 0.09	Tumor necrosis factor receptor superfamily, member 5
	tnf	–	−2.53 ± 0.06	Tumor necrosis factor (*tnf* superfamily, member 2)
GO:0007165, signal transduction	*arhgap22*	–	+2.07 ± 0.8	Rho GTPase activating protein 22
	rhov	–	+2.17 ± 0.05	ras homolog gene family, member V
GO:0003824, catalytic activity	*atg16l1*	–	+2.30 ± 0.03	atg16 autophagy related 16-like 1
GO:0001664, G-protein coupled receptor binding	*apln*	–	+2.20 ± 0.09	Apelin
GO:0003700, transcription factor activity	*nfκb2*	–	−2.61 ± 0.04	Nuclear factor of kappa light polypeptide gene enhancer in B-cells 2 (p49/p100)
GO: response to oxidative stress	*gclc*	–	+2.53 ± 0.04	*Rattus norvegicus* glutamate-cysteine ligase, catalytic subunit

[a] Gene ontology terms.

Table 3
Incidence of nanoparticles on gene expression as measured by RT-qPCR ($p \leq 0.01$).

Approved gene symbol	Fold change ± SD	
	NP/ERS (25 μg/mL)	NP/ERS (100 μg/mL)
pdcd4	−1.22 ± 0.07	−2.10 ± 0.08
bcl2	−1.29 ± 0.06	−2.00 ± 0.05
casp8	−0.85 ± 0.04	−1.90 ± 0.03
opa1	−1.35 ± 0.05	−2.45 ± 0.04
tnf	−1.00 ± 0.02	−1.80 ± 0.08
nfκb2	−1.76 ± 0.07	−2.28 ± 0.05
atg16l1	+19.20 ± 0.92	+17.45 ± 0.68
ncf1	+4.78 ± 0.14	+9.82 ± 0.29

− and + indicate under- and up-expression, respectively as compared to untreated cells.

and more pronounced in 100 μg/mL treated cells. The exposure of cells to nanoparticles at a concentration of 100 μg/mL resulted in the down regulation of the *opa1* gene, of the two anti-apoptotic genes *bcl2l13* and *nfκb2* and of the bifunctional apoptosis regulator (*bfar*) as well as of the pro-apototic genes *casp8* and *pdcd4*. On the contrary, the *tnfrsf5* genes (TNF receptor superfamily member 5 and cd40), the anti-apoptotic genes [*rhov* and *arhgap22* (a rho GTPase activating protein), *rtkn* (the rho effector rhotekin) and *apln* (apelin related to G-proteins)] as well as *atg16l1 a* pro-autophagic gene encoding for a protein belonging to a large protein complex necessary for autophagy (Saitoh et al., 2008), were up regulated. The gene of the glutamate-cysteine ligase (a key gene in the glutathione homeostasis) catalytic subunit (*gclc*) was also up regulated in cells treated with 100 μg/mL NP/ERS (Table 2).

3.4. qRT-PCR

qRT-PCR confirmed the microarray data indicating a down-expression of *opa1*, *bcl2l13*, *pdcd4*, *casp8*, *tnf* and *nfκb2* in 100 μg/mL particle-treated cells (Table 3). Our results showed also a significant up regulation of *atg16l1* in cells treated with 25 and 100 μg/mL of NP/ERS (Table 3). Additionally, a dose-dependent up regulation of *ncf1* (neutrophil cytosolic factor 1), an $O_2^{\bullet -}$ generating enzyme, was evidenced (Table 3)

3.5. Western blot

Western blot showed a time- and dose-dependent decrease of OPA1 and NFκB protein content in cells exposed to 100 μg/mL NP (Fig. 3d and e). In agreement with up regulation of the autophagy *atg16l1* gene, above reported, the conversion of microtubule-associated protein 1 light chain 3 (LC3) into the LC3-II isoform, a common autophagy marker (Asanuma et al., 2003), was also detected in nanoparticle exposed cells (Fig. 4b). Additionally, no poly(ADP-ribose) polymerase (PARP) protein fragmentation was detected in the NP/ERS-treated cells whatever the nanoparticle concentration (data not shown).

3.6. Immunofluorescence assay

Treatment of NR8383 with NP/ERS at a final concentration of 25, 50 and 100 μg/mL for 4 h induced a dose-dependent accumulation of LC3-positive vesicles (Fig. 4c).

3.7. Intracellular GSH

Our data showed a significant decrease of intracellular reduced GSH (∼52%) in cells treated with the higher concentration of NP/ERS, 100 μg/mL for 24 h, as compared to control (Fig. 5).

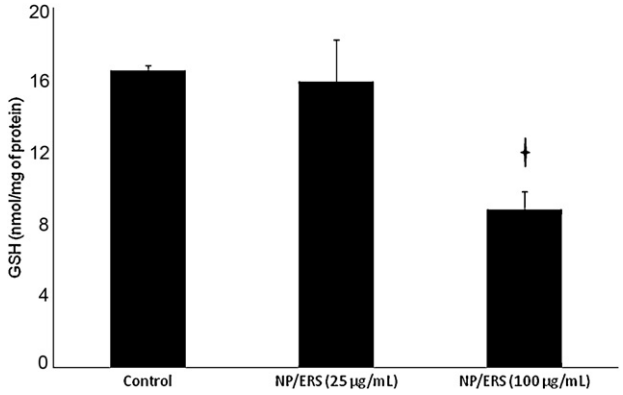

Fig. 5. The decrease of intracellular reduced GSH level in NR8383 cells exposed to 25 and 100 μg/mL of NP/ERS for 24 h. Data were expressed as nmol of GSH per mg of protein. Dagger indicates a significant difference at $p \leq 0.01$.

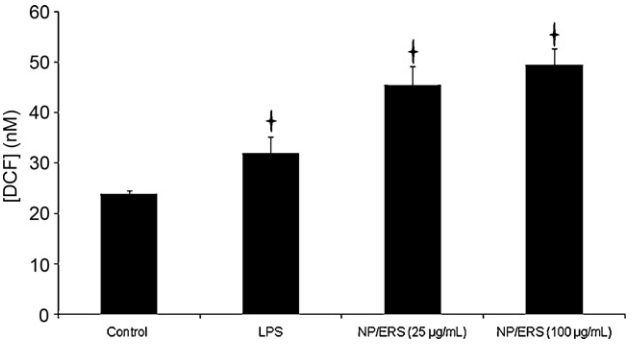

Fig. 6. Intracellular ROS level increase in NR8383 cells after a 24 h exposure to NP/ERS. LPS (1 μg/mL) is used as a ROS inducer. Dagger indicates a significant difference at $p \leq 0.01$.

3.8. ROS production

A significant increase of ROS production ratio, expressed by DCF concentration (nM), was evidenced in cells incubated with 25 (∼1.9 times) and 100 μg/mL (∼2.1 times) of NP/ERS for 24 h as compared to unexposed cells (Fig. 6).

4. Discussion

4.1. NP/ERS uptake by NR8383 macrophages and mitochondria targeting

It has been reported that endocytosis pathway plays a fundamental role in a wide range of cellular function; in particular it affects the functions of mitochondria (Polo and Di Fiore, 2006). Uptake of particles by endocytosis depends primarily on their size and ionic charge (Xia et al., 2006). It has been documented that cationic and small diameter nanoparticles, such as 60 nm NH_2-labeled nanospheres, are internalized into the cells and gain access to cellular organelles and may damage mitochondria. On the contrary, anionic and larger nanoparticles of 200 nm diameter do not (Xia et al., 2006, 2008). In addition, it has been reported that single-walled carbon nanotubes (SWCNTs), which are known to induce cytotoxicity, target the mitochondria (Yang et al., 2010). In line with these evidences, in our study we observed numerous NP/ERS in the vicinity of the inner mitochondria membrane. Among the genes responsible of mitochondria functions, *opa1* gene plays a major role in the maintenance of the mitochondrial network morphology and dynamics and in the regulation of the signal pathways of cellular death (Chen et al., 2003). In fact, *opa1* was reported to play this

role along with *mfn1* and *mfn2* genes, of which respective products mitofusin1 and 2, are mediators of mitochondrial fusion. In retinal ganglial cells, a down regulation of *opa1* has been reported to promote the aggregation of the mitochondrial network and to alter the structure of the mitochondrial inner membrane (Kamei et al., 2005). In particular the disorganization of the *cristae*, the release of cytochrome *c* and the induction of intrinsic apoptosis has been observed (Arnoult et al., 2005; Olichon et al., 2003). In our study, *opa1* down regulation as well as electron microscopy observations suggest that NP/ERS cytotoxicity in macrophages is triggered by their effect on mitochondria. However, it is difficult to determine whether nanoparticles induce the mitochondrial decay by altering gene expression or by a mechanical impairment, e.g. by abolishing transmembrane proton gradient.

4.2. Oxidative stress induction by ERS nanoparticles

Damage to the mitochondrial inner membrane, caused by *opa1* down expression, increases ROS production that causes further lysosomal disruption (Arnoult et al., 2005). This disruption could liberate nanoparticles enclosed in endocytic vesicles which eventually reach their target, namely the mitochondria and penetrate them triggering the autophagy process. These data suggest that crosstalk between the lysosome and mitochondria could play an important role in determining cell death type. Intracellular reactive oxygen species (ROS) production as well as oxidative stress occurs in NP/ERS-treated cells. In fact, by using qRT-PCR assays we observed the over expression of both *ncf1*, a gene encoding a subunit of NADPH oxidase (Dika Nguea et al., 2008), and of *gclc*, one of the key genes responsible for GSH homeostasis (Dickinson et al., 2004). In agreement with these data, in NP/ERS-treated cells we evidenced a significant decrease of the cellular concentration of reduced glutathione (GSH) and an increase of ROS production.

4.3. Apoptosis inhibition by NP/ERS

Treatment of NR8383 cells with NP/ERS nanoparticles does not induce apoptotic cellular death. In our previous work, we have shown the absence of apoptotic processes that was ascertained by the facts that neither the poly(ADP-ribose) polymerase (PARP) fragmentation nor the formation of DNA laddering was observed. However, histochemical assays indicate the activation of caspase 3 and caspase 7 (Eidi et al., 2010). Although many reports indicate that *tnf* expression was elevated by nanoparticle treatment (Chen et al., 2006; Minematsu et al., 2007), there are contradictory data on its expression due to the use of different experimental cell models (Niu et al., 2007). TNF receptor superfamily member 5 (*tnfrsf5*), known as a potent inhibitor of *nfκb2* gene expression in dendritic cells (Mann et al., 2002) affecting the extrinsic apoptosis pathway (Wallach et al., 1997), was up regulated in our experiment. It has been proved also that *tnf* is able to induce extrinsic apoptosis through the *casp8* activation pathway that was under expressed in our study (Bhattacharyya et al., 2010). Evidence of suppression of the cellular signaling pathway leading to extrinsic apoptosis was obtained in our study by the down regulation of proapoptotic genes, e.g. *pdcd4* (Vikhreva et al., 2010), *casp8* and *bcl2L13* (Talotta et al., 2009). Furthermore, genes involved in extrinsic apoptosis inhibition were up regulated like *rhov*, *arhgap22*, *rtkn* and *apln*. Those data are not in favor of an underlying extrinsic apoptosis process triggered by nanoparticles and we explored further the intrinsic apoptosis. In fact, a possible activation of intrinsic apoptosis is supported by microarray and qRT-PCR assays which show the down regulation of *opa1*, *nfκb2*, *bcl2*. Indeed, some reports have indicated that *nfκb2* induced *bcl2* expression and promoted cell survival (Oberdorster et al., 2005; Viatour et al., 2003). Furthermore, the bifunctional apoptosis regulator (*bfar*), an inhibitor of BAX-induced apoptosis (Zhang et al., 2000), was down-regulated in our experiment. Interestingly, our data showed that neither extrinsic nor intrinsic apoptotic cell death pathways are activated in NR/ERS-treated cells. Instead NR/ERS seem to lead the cells toward the autophagic cell death.

4.4. ERS nanoparticles induce autophagy

An inverse relationship between the activation of the genes involved in the apoptosis and those involved in the autophagy, which may corresponds to a switch from apoptosis to autophagy, has been described (Luo and Rubinsztein, 2007; Shimizu et al., 2004). In particular a decrease in the expression of the apoptotic *bcl* family genes and the activation of the autophagic *atg* family genes has been reported. In our system we observe a decreased expression of *bcl2*, an efficient autophagy inhibitor (Sasi et al., 2009) and an over expression of *atg16l1* as well as the conversion of the microtubule-associated protein 1 light chain 3 (LC3) into the LC3-II isoform, a common marker of autophagy (Asanuma et al., 2003). Moreover, we report the down regulation of proautophagic gene, namely *casp8* that was reported to induce autophagy cell death in U937 macrophages (Yu et al., 2004). Furthermore, we observed cellular alterations characteristic of autophagic cell death: phagophores, autophagosomes and "mitophagy". Such morphological modifications have been described recently in cells treated with gold nanoparticles (Li et al., 2010), soluble fullerenes (Yamawaki and Iwai, 2006), viruses (Sir and Ou, 2008), quantum dots (Seleverstov et al., 2006) and SWCNTs (Yang et al., 2010). Through autophagy, cells not only recycle intracellular components and compensate for nutrient deprivation but also they eliminate selectively damaged organelles/proteins and maintain cellular homeostasis. Non-selective autophagy degrades all organelles and long-lived proteins to provide the energy required for cell survival. By contrast, mitophagy selectively eliminates mitochondria to regulate their number as well as to remove specifically the damaged ones (Youle and Narendra, 2011). Our results demonstrate that NP/ERS-mediated cell toxicity occurs *via* organelle, notably mitochondrion, autophagy which amplifies a physiological process. In a future work, it would be interesting to study the cytotoxicity and cell morphological modifications occurring after longer exposure of macrophages with lower doses.

5. Conclusion

Nanotechnology has attracted increasing interest among almost all fields of research. Notable improvements in our knowledge about metallic nano-objects or carbon nanotubes toxicity and their influence on the expression of genes and the impairment of the oxidant/antioxidant cellular balance have been obtained. Nevertheless, data on the toxicity of drug delivery nanoparticles remain extremely scarce. To the best of our knowledge, this article is the first to report that polymeric nanoparticles designed for drug delivery, upon their enclosure into macrophages by endocytosis, are able to cross the mitochondrial membranes and enter inside these organelles. This process induces a cascade of events such as the unbalance of the oxidant/antioxidant homeostasis and the modification of the expression of genes and proteins, especially those implied in macrophages activation and autophagy. As a consequence, a mitochondrial decay through phagophore and autophagosome formation and eventually mitophagy occurs. How immune cells deal with nanoparticles is an interesting issue as this process presents some analogy with viral infections. Furthermore, the identification of the early cellular markers described and discussed in this article may serve as a conceptual scaffold for designing experiments for a better understanding of the cellular

toxicity of loaded and unloaded nanoparticles. The evaluation of cytotoxic effects in term of autophagy is a rather new concept but it should be investigated for every type of carrier to be used for drug delivery. As we have used a model of rat macrophages, human derived cell lines as well as in vivo models should be also tested to confirm these results.

Acknowledgements

The authors thank Dr. Lucia Marcocci for her help and support in reviewing the manuscript. Authors would like to acknowledge Lu Zhang, Kevin Dalleau, Bouchra Mouaraki, Christine Manencq and Ramia Safar for their kind help in microarray and PCR experiments.

References

Arnoult, D., Grodet, A., Lee, Y.J., Estaquier, J., Blackstone, C., 2005. Release of OPA1 during apoptosis participates in the rapid and complete release of cytochrome c and subsequent mitochondrial fragmentation. J. Biol. Chem. 280, 35742–35750.

Asanuma, K., Tanida, I., Shirato, I., Ueno, T., Takahara, H., Nishitani, T., Kominami, E., Tomino, Y., 2003. MAP-LC3, a promising autophagosomal marker, is processed during the differentiation and recovery of podocytes from PAN nephrosis. FASEB J. 17, 1165–1167.

Bhardwaj, P., Chaurasia, H., Chaurasia, D., Prajapati, S.K., Singh, S., 2010. Formulation and in-vitro evaluation of floating microballoons of indomethacin. Acta Pol. Pharm. 67, 291–298.

Bhattacharyya, S., Dudeja, P.K., Tobacman, J.K., 2010. Tumor necrosis factor alpha-induced inflammation is increased but apoptosis is inhibited by common food additive carrageenan. J. Biol. Chem. 285, 39511–39522.

Bodmeier, R., Chen, H., Tyle, P., Jarosz, P., 1991. Spontaneous formation of drug-containing acrylic nanoparticles. J. Microencapsul. 8, 161–170.

Brazma, A., Hingamp, P., Quackenbush, J., Sherlock, G., Spellman, P., Stoeckert, C., Aach, J., Ansorge, W., Ball, C.A., Causton, H.C., Gaasterland, T., Glenisson, P., Holstege, F.C., Kim, I.F., Markowitz, V., Matese, J.C., Parkinson, H., Robinson, A., Sarkans, U., Schulze-Kremer, S., Stewart, J., Taylor, R., Vilo, J., Vingron, M., 2001. Minimum information about a microarray experiment (MIAME)-toward standards for microarray data. Nat. Genet. 29, 365–371.

Chen, H., Detmer, S.A., Ewald, A.J., Griffin, E.E., Fraser, S.E., Chan, D.C., 2003. Mitofusins Mfn1 and Mfn2 coordinately regulate mitochondrial fusion and are essential for embryonic development. J. Cell Biol. 160, 189–200.

Chen, H.W., Su, S.F., Chien, C.T., Lin, W.H., Yu, S.L., Chou, C.C., Chen, J.J., Yang, P.C., 2006. Titanium dioxide nanoparticles induce emphysema-like lung injury in mice. FASEB J. 20, 2393–2395.

Corcelle, E., Nebout, M., Bekri, S., Gauthier, N., Hofman, P., Poujeol, P., Fenichel, P., Mograbi, B., 2006. Disruption of autophagy at the maturation step by the carcinogen lindane is associated with the sustained mitogen-activated protein kinase/extracellular signal-regulated kinase activity. Cancer Res. 66, 6861–6870.

Dickinson, D.A., Levonen, A.L., Moellering, D.R., Arnold, E.K., Zhang, H., Darley-Usmar, V.M., Forman, H.J., 2004. Human glutamate cysteine ligase gene regulation through the electrophile response element. Free Radic. Biol. Med. 37, 1152–1159.

Dika Nguea, H., de Reydellet, A., Lehuede, P., De Meringo, A., Le Faou, A., Marcocci, L., Rihn, B.H., 2008. Gene expression profile in monocyte during in vitro mineral fiber degradation. Arch. Toxicol. 82, 355–362.

Eidi, H., Joubert, O., Attik, G., Duval, R.E., Bottin, M.C., Hamouia, A., Maincent, P., Rihn, B.H., 2010. Cytotoxicity assessment of heparin nanoparticles in NR8383 macrophages. Int. J. Pharm.

Fessi, H., Puisieux, F., 1989. Nanocapsule formation by interfacial polymer deposition following solvent displacement. Int. J. Pharm. 55, 1–4.

Gargouri, M., Sapin, A., Bouli, S., Becuwe, P., Merlin, J.L., Maincent, P., 2009. Optimization of a new non-viral vector for transfection: Eudragit nanoparticles for the delivery of a DNA plasmid. Technol. Cancer Res. Treat. 8, 433–444.

Hoffart, V., Lamprecht, A., Maincent, P., Lecompte, T., Vigneron, C., Ubrich, N., 2006. Oral bioavailability of a low molecular weight heparin using a polymeric delivery system. J. Control. Release 113, 38–42.

Jiao, Y., Ubrich, N., Marchand-Arvier, M., Vigneron, C., Hoffman, M., Lecompte, T., Maincent, P., 2002. In vitro and in vivo evaluation of oral heparin-loaded polymeric nanoparticles in rabbits. Circulation 105, 230–235.

Kamei, S., Chen-Kuo-Chang, M., Cazevieille, C., Lenaers, G., Olichon, A., Belenguer, P., Roussignol, G., Renard, N., Eybalin, M., Michelin, A., Delettre, C., Brabet, P., Hamel, C.P., 2005. Expression of the Opa1 mitochondrial protein in retinal ganglion cells: its downregulation causes aggregation of the mitochondrial network. Invest. Ophthalmol. Vis. Sci. 46, 4288–4294.

Laemmli, U.K., 1970. Cleavage of structural proteins during the assembly of the head of bacteriophage T4. Nature 227, 680–685.

Lamprecht, A., Koenig, P., Ubrich, N., Maincent, P., Neumann, D., 2006. Low molecular weight heparin nanoparticles: mucoadhesion and behaviour in Caco-2 cells. Nanotechnology 17, 3673–3680.

Lewicki, K., Marchand, S., Matoub, L., Lulek, J., Coulon, J., Leroy, P., 2006. Development of a fluorescence-based microtiter plate method for the measurement of glutathione in yeast. Talanta 70, 876–882.

Li, J.J., Hartono, D., Ong, C.N., Bay, B.H., Yung, L.Y., 2010. Autophagy and oxidative stress associated with gold nanoparticles. Biomaterials 31, 5996–6003.

Lin, Z., Fillmore, G.C., Um, T.H., Elenitoba-Johnson, K.S., Lim, M.S., 2003. Comparative microarray analysis of gene expression during activation of human peripheral blood T cells and leukemic Jurkat T cells. Lab. Invest. 83, 765–776.

Lowry, O.H., Rosebrough, N.J., Farr, A.L., Randall, R.J., 1951. Protein measurement with the Folin phenol reagent. J. Biol. Chem. 193, 265–275.

Luo, S., Rubinsztein, D.C., 2007. Atg5 and Bcl-2 provide novel insights into the interplay between apoptosis and autophagy. Cell Death Differ. 14, 1247–1250.

Mann, J., Oakley, F., Johnson, P.W., Mann, D.A., 2002. CD40 induces interleukin-6 gene transcription in dendritic cells: regulation by TRAF2, AP-1, NF-kappa B, and CBF1. J. Biol. Chem. 277, 17125–17138.

Minematsu, H., Shin, M.J., Celil Aydemir, A.B., Seo, S.W., Kim, D.W., Blaine, T.A., Macian, F., Yang, J., Young-In Lee, F., 2007. Orthopedic implant particle-induced tumor necrosis factor-alpha production in macrophage-monocyte lineage cells is mediated by nuclear factor of activated T cells. Ann. N. Y. Acad. Sci. 1117, 143–150.

Nguea, H.D., de Reydellet, A., Le Faou, A., Zaiou, M., Rihn, B., 2008. Macrophage culture as a suitable paradigm for evaluation of synthetic vitreous fibers. Crit. Rev. Toxicol. 38, 675–695.

Niu, J., Azfer, A., Rogers, L.M., Wang, X., Kolattukudy, P.E., 2007. Cardioprotective effects of cerium oxide nanoparticles in a transgenic murine model of cardiomyopathy. Cardiovasc. Res. 73, 549–559.

Oberdorster, G., Maynard, A., Donaldson, K., Castranova, V., Fitzpatrick, J., Ausman, K., Carter, J., Karn, B., Kreyling, W., Lai, D., Olin, S., Monteiro-Riviere, N., Warheit, D., Yang, H., 2005. Principles for characterizing the potential human health effects from exposure to nanomaterials: elements of a screening strategy. Part Fibre Toxicol. 2, 8.

Olichon, A., Baricault, L., Gas, N., Guillou, E., Valette, A., Belenguer, P., Lenaers, G., 2003. Loss of OPA1 perturbates the mitochondrial inner membrane structure and integrity, leading to cytochrome c release and apoptosis. J. Biol. Chem. 278, 7743–7746.

Pignatello, R., Bucolo, C., Ferrara, P., Maltese, A., Puleo, A., Puglisi, G., 2002. Eudragit RS100 nanosuspensions for the ophthalmic controlled delivery of ibuprofen. Eur. J. Pharm. Sci. 16, 53–61.

Polo, S., Di Fiore, P.P., 2006. Endocytosis conducts the cell signaling orchestra. Cell 124, 897–900.

Saitoh, T., Fujita, N., Jang, M.H., Uematsu, S., Yang, B.G., Satoh, T., Omori, H., Noda, T., Yamamoto, N., Komatsu, M., Tanaka, K., Kawai, T., Tsujimura, T., Takeuchi, O., Yoshimori, T., Akira, S., 2008. Loss of the autophagy protein Atg16L1 enhances endotoxin-induced IL-1beta production. Nature 456, 264–268.

Sasi, N., Hwang, M., Jaboin, J., Csiki, I., Lu, B., 2009. Regulated cell death pathways: new twists in modulation of BCL2 family function. Mol. Cancer Ther. 8, 1421–1429.

Schaffazick, S.R., Siqueira, I.R., Badejo, A.S., Jornada, D.S., Pohlmann, A.R., Netto, C.A., Guterres, S.S., 2008. Incorporation in polymeric nanocapsules improves the antioxidant effect of melatonin against lipid peroxidation in mice brain and liver. Eur. J. Pharm. Biopharm. 69, 64–71.

Seleverstov, O., Zabirnyk, O., Zscharnack, M., Bulavina, L., Nowicki, M., Heinrich, J.M., Yezhelyev, M., Emmrich, F., O'Regan, R., Bader, A., 2006. Quantum dots for human mesenchymal stem cells labeling. A size-dependent autophagy activation. Nano Lett. 6, 2826–2832.

Shimizu, S., Kanaseki, T., Mizushima, N., Mizuta, T., Arakawa-Kobayashi, S., Thompson, C.B., Tsujimoto, Y., 2004. Role of Bcl-2 family proteins in a non-apoptotic programmed cell death dependent on autophagy genes. Nat. Cell Biol. 6, 1221–1228.

Sir, D., Ou, J.H., 2008. Autophagy in viral replication and pathogenesis. Mol. Cells 29, 1–7.

Suri, S.S., Fenniri, H., Singh, B., 2007. Nanotechnology-based drug delivery systems. J. Occup. Med. Toxicol. 2, 16.

Talotta, F., Cimmino, A., Matarazzo, M.R., Casalino, L., De Vita, G., D'Esposito, M., Di Lauro, R., Verde, P., 2009. An autoregulatory loop mediated by miR-21 and PDCD4 controls the AP-1 activity in RAS transformation. Oncogene 28, 73–84.

Unger, F., Wittmar, M., Kissel, T., 2007. Branched polyesters based on poly[vinyl-3-(dialkylamino)alkylcarbamate-co-vinyl acetate-co-vinyl alcohol]-graftpoly(D,L-lactide-co-glycolide): effects of polymer structure on cytotoxicity. Biomaterials 28, 1610–1619.

Viatour, P., Bentires-Alj, M., Chariot, A., Deregowski, V., de Leval, L., Merville, M.P., Bours, V., 2003. NF- kappa B2/p100 induces Bcl-2 expression. Leukemia 17, 1349–1356.

Vikhreva, P.N., Shepelev, M.V., Korobko, E.V., Korobko, I.V., 2010. Pdcd4 tumor suppressor: properties, functions, and their application to oncology. Mol. Gen. Mikrobiol. Virusol., 3–11.

Wallach, D., Boldin, M., Varfolomeev, E., Beyaert, R., Vandenabeele, P., Fiers, W., 1997. Cell death induction by receptors of the TNF family: towards a molecular understanding. FEBS Lett. 410, 96–106.

Wang, H., Joseph, J.A., 1999. Quantifying cellular oxidative stress by dichlorofluorescein assay using microplate reader. Free Radic. Biol. Med. 27, 612–616.

Xia, T., Kovochich, M., Brant, J., Hotze, M., Sempf, J., Oberley, T., Sioutas, C., Yeh, J.I., Wiesner, M.R., Nel, A.E., 2006. Comparison of the abilities of ambient and manufactured nanoparticles to induce cellular toxicity according to an oxidative stress paradigm. Nano Lett. 6, 1794–1807.

Xia, T., Kovochich, M., Liong, M., Zink, J.I., Nel, A.E., 2008. Cationic polystyrene nanosphere toxicity depends on cell-specific endocytic and mitochondrial injury pathways. ACS Nano 2, 85–96.

Yamawaki, H., Iwai, N., 2006. Cytotoxicity of water-soluble fullerene in vascular endothelial cells. Am. J. Physiol. Cell Physiol. 290, C1495–C1502.
Yang, Z., Zhang, Y., Yang, Y., Sun, L., Han, D., Li, H., Wang, C., 2010. Pharmacological and toxicological target organelles and safe use of single-walled carbon nanotubes as drug carriers in treating Alzheimer disease. Nanomedicine 6, 427–441.
Youle, R.J., Narendra, D.P., 2011. Mechanisms of mitophagy. Nat. Rev. Mol. Cell Biol. 12, 9–14.
Yu, L., Alva, A., Su, H., Dutt, P., Freundt, E., Welsh, S., Baehrecke, E.H., Lenardo, M.J., 2004. Regulation of an ATG7-beclin 1 program of autophagic cell death by caspase-8. Science 304, 1500–1502.
Zhang, H., Xu, Q., Krajewski, S., Krajewska, M., Xie, Z., Fuess, S., Kitada, S., Pawlowski, K., Godzik, A., Reed, J.C., 2000. BAR: an apoptosis regulator at the intersection of caspases and Bcl-2 family proteins. Proc. Natl. Acad. Sci. U.S.A. 97, 2597–2602.